doi: 10.82124/CEAS-GNC-2026-043 CEAS-GNC-2026-043

Probabilistic Robustness Analysis of Satellite Attitude Control Using Polynomial Chaos

Markus Lötzsch Research Assistant, Technische Universität Dresden, Chair of Flight Mechanics and Control, 01062 Dresden, Germany. markus.loetzsch@tu-dresden.de

Emily Burgin Research Assistant, Technische Universität Dresden, Chair of Flight Mechanics and Control, 01062 Dresden, Germany. emily.burgin@tu-dresden.de

Maurice Martin AOCS/GNC Design and Analysis Engineer, Airbus Defence and Space GmbH, Claude-Dornier-Str., 88090 Immenstaad, Germany. maurice.martin@airbus.com

Stefan Winkler Honorary Professor, Senior Expert in Spacecraft Autonomy, Navigation & Control, Airbus Defence and Space GmbH, Claude-Dornier-Str., 88090 Immenstaad, Germany. stefan.st.winkler@airbus.com

Harald Pfifer Professor, Technische Universität Dresden, Chair of Flight Mechanics and Control, 01062 Dresden, Germany. harald.pfifer@tu-dresden.de

ABSTRACT

This paper presents an approach for the probabilistic analysis of stability margins and pointing errors for a satellite system subject to parametric uncertainties. To analyze the influence of the uncertainties on the system performance, probabilistic approaches provide more convincing insights than worst-case methods. The classical approach uses Monte Carlo simulations which come with high computational effort. As an alternative, we apply non-intrusive Polynomial Chaos Expansion, which approximates a function of stochastic arguments as a series of orthogonal basis polynomials. To deal with a high-dimensional uncertainty space, sparse grid quadrature is employed to calculate the coefficients of the polynomial system. We show that Polynomial Chaos Expansion can replicate the results of Monte Carlo simulations with almost perfect accuracy, while requiring 20-30 times lower computation times. The non-intrusive approach also allows flexible evaluation of various quantities of interest, proving the applicability of this method in the industrial Verification and Validation process.

Keywords: Polynomial Chaos Expansion, Robustness Analysis, Sparse Grids, Satellite Attitude Control

Nomenclature

δ	=	Uncertain parameter vector
y_α	=	PCE coefficients
ψ_α	=	PCE basis polynomials
γ_α	=	L_2-norm of basis polynomial
w	=	Weighting function
A, B, C, D	=	State space matrices

x	=	State vector
u	=	Input vector
y	=	Output vector
$n, \cdot_n$	=	Noise
$d, \cdot_d$	=	Disturbance
z	=	Error metric
$\mathbb{E}[\cdot]$	=	Expected value
$\mathrm{Var}[\cdot]$	=	Variance
$\mathcal{U}$	=	Univariate quadrature rule
$\boldsymbol{Q}$	=	Multivariate quadrature rule
$\langle \cdot, \cdot \rangle$	=	Inner product
$\otimes$	=	Tensor product
μ	=	Mean
σ	=	Standard deviation
$\hat{\cdot}$	=	Sampled quantity

1 Introduction

The verification and validation (V&V) of space vehicle control systems is a challenging and resource-intensive process. The complex nature of the systems and a potentially large number of uncertain parameters pose difficulties in assessing the performance and robustness requirements. The existing approaches can be categorized in deterministic (i.e. worst-case) and probabilistic methods [1].

This paper contributes a computationally efficient probabilistic approach based on the concept of Polynomial Chaos Expansion (PCE) to calculate stability margins and pointing metrics for satellite attitude control. We demonstrate that PCE can provide accurate statistical characterizations of the system across the entire uncertainty space. By systematically comparing PCE with conventional probabilistic analysis using Monte Carlo (MC) simulations, we highlight the significant reduction in computational effort offered by PCE.

Classical deterministic and probabilistic methods both come with their own challenges: For the first, it is hard to verify that the worst case configuration has really been achieved [1] and models might be invalidated based on worst-case events that are unlikely in a practical setting [2]. Additionally, it has been shown that a controller based on a worst-case approach can have a higher overall risk of destabilizing a system compared to a controller based on probabilistic metrics [3]. Hence, it is desirable to know the distribution of stability margins and performance metrics subject to random parameters. MC simulations are the industry standard to generate such distributions because of the straight-forward implementation. A large number of random samples are drawn from the uncertain parameters according to their probability distribution and the resulting system behavior is simulated. Statistical moments such as mean and variance of the quantities of interest can be calculated from their sampled distribution and a probability function can be fitted. However, they are typically limited by their high computational cost [1]. Recently, combining traditional deterministic methods, namely the structured singular value, with probabilistic assessments, see [2], have been promising. Still, they come at a large computational burden for complex industrial models and usually rely on model simplification or reduction.

The computational effort of MC motivates the exploration of more efficient uncertainty quantification techniques. Methods based on Polynomial Chaos Expansion (PCE) have attracted increasing interest in the probabilistic analysis of uncertain systems. PCE offers a computationally efficient alternative by representing system responses as spectral expansions in terms of orthogonal polynomials of the input

uncertainties. This formulation yields direct access to statistical moments and enables fast sampling, significantly reducing computational costs in uncertainty propagation. Those properties allow for time and resource savings in the design and V&V process. Examples of the successful application of PCE in the aerospace sector include the verification of satellite acquisition sequences [4], robustness analysis of an automatic landing system [5] or the trajectory optimization of launch vehicles [6].

In this work, we apply a PCE-based framework on a satellite attitude controller for the MetOp Second Generation spacecraft. We perform a probabilistic analysis of the gain and phase margins and the absolute pointing error metric under a high-dimensional uncertainty space. The results are then compared to MC simulations of appropriate sample size, both regarding accuracy and computation times.

2 Background

2.1 Uncertain Linear Time-Invariant Systems

Consider an linear time-invariant (LTI) system whose state space matrices are subject to stochastic uncertain parameters δ:

$$\begin{bmatrix} \dot{x}(t,\delta) \\ y(t,\delta) \end{bmatrix} = \begin{bmatrix} A(\delta) & B(\delta) \\ C(\delta) & D(\delta) \end{bmatrix} \begin{bmatrix} x(t,\delta) \\ u(t) \end{bmatrix} \tag{1}$$

where $\delta \in \Delta^{n_\delta}$ is a unknown time-invariant parameter vector bounded within a compact subset $\Delta^{n_\delta} \subset \mathbb{R}^{n_\delta}$ subject to a known probability distribution $p(\delta)$. The state space matrices $A : \Delta^{n_\delta} \to \mathbb{R}^{n_x \times n_x}$, $B : \Delta^{n_\delta} \to \mathbb{R}^{n_x \times n_u}$, $C : \Delta^{n_\delta} \to \mathbb{R}^{n_y \times n_x}$, $D : \Delta^{n_\delta} \to \mathbb{R}^{n_y \times n_u}$ define the relation between the state vector $x(t,\delta) \in \mathbb{R}^{n_x}$, the input vector $u(t) \in \mathbb{R}^{n_u}$ and the output vector $y(t,\delta) \in \mathbb{R}^{n_y}$. The stability margins and compliance with the pointing requirements must be assessed for all $\delta \in \Delta^{n_\delta}$.

2.2 Polynomial Chaos Expansion

The idea of PCE was first introduced by Wiener [7] in 1938. Consider the probability space $(\Omega, \mathcal{F}, P)$ where Ω is the sample space, $\mathcal{F}$ is the event space and P is a probability function, and a vector of random variables $\delta : \Omega \to \mathbb{R}^{n_\delta}$. A function $Y(\delta)$ with finite variance depending on a random variable can then be decomposed in a series of orthogonal basis functions ψ_α [8]. For simplicity, the case with $n_\delta = 1$, resulting in univariate basis polynomials is defined first and later expanded to multivariate polynomials:

$$Y(\delta) = \sum_{\alpha=0}^{\infty} y_\alpha \psi_\alpha(\delta) \tag{2}$$

The basis functions fulfill the orthogonality condition

$$\langle \psi_\alpha, \psi_\beta \rangle := \int_{\mathcal{D}} \psi_\alpha(x)\psi_\beta(x)w(x)\mathrm{d}x = \begin{cases} \gamma_\alpha^2 & \text{if } \alpha = \beta \\ 0 & \text{otherwise} \end{cases} \quad \forall \alpha, \beta \in \mathbb{N}_0 \tag{3}$$

where $w(x)$ is a weighting function and γ_α is the L_2-norm of ψ_α. For practical applications, the infinite series in Eq. 2 is truncated to include only L terms:

$$Y(\delta) \approx \sum_{\alpha=0}^{L-1} y_\alpha \psi_\alpha(\delta) \tag{4}$$

Wiener originally only considered Hermite polynomials as basis functions that correspond to normal distributed random variables. Later, this system was expanded to other probability distributions by

choosing adequate polynomials whose weighting function $w(x)$ correspond to the probability density function (PDF) of the respective distribution. By selecting the correct polynomial basis, an exponential convergence rate with respect to the maximum polynomial degree $L-1$ can be achieved for sufficiently smooth model responses (Tab. 1) [9].

Table 1 Polynomial basis for different probability distributions

probability distribution	weighting function	polynomial	support
gaussian	$e^{-x^2/2}$	Hermite	$(-\infty, \infty)$
uniform	1	Legendre	$[-1, 1]$
beta	$(1-x)^{\alpha}(1-x)^{\beta}$	Jacobi	$[-1, 1]$
gamma	e^{-x}	Laguerre	$[0, \infty)$

The resulting expanded polynomial system has two important properties with respect to the stochastic analysis of the output. First, the expected value $\mathbb{E}[\cdot]$ and variance $\mathrm{Var}[\cdot]$ can be directly computed from the coefficients y_α:

$$\mathbb{E}[Y(\delta)] \approx y_0, \ \mathrm{Var}[Y(\delta)] \approx \sum_{\alpha=1}^{L-1} y_\alpha^2 \langle \psi_\alpha^2 \rangle \tag{5}$$

where $\langle \psi_\alpha^2 \rangle = \gamma_\alpha^2$ has a simple, closed form expression depending on the chosen polynomial basis. Second, instead of simulating the behavior of the original system for different samples of δ, the polynomial expression in Eq. 4 can be evaluated for the same samples, which is generally significantly more efficient. PCE methods are commonly classified into two categories: intrusive and non-intrusive approaches. For intrusive approaches, the terms in the model equations that depend on the uncertain parameter are directly substituted by series expansions of suitable basis polynomials corresponding to the distribution of the parameter. That leads to a system of coupled differential equations that must be solved to obtain the coefficients. Systems that contain complicated (especially non-polynomial) functions can make the computation of the coefficients prohibitive or impossible [10] and the exact model equations must be available. In contrast, non-intrusive PCE, as discussed below, treats the model as a black box. Only the output of an arbitrary function of the uncertain parameters at certain nodal points is required for calculating the coefficients, while the function definition itself can remain unknown. Consider a function $Y(\delta)$ that is expanded as an truncated series as in Eq. 4. To calculate the k-th coefficient y_k, both sides are multiplied by ψ_k and the inner product $\langle \cdot, \cdot \rangle$ is taken. Because of the orthogonality condition (Eq. 3), all summands except for $y_k \psi_k \psi_k$ become zero:

$$\langle Y(\delta), \psi_k(\delta) \rangle \approx \langle y_k, \psi_k(\delta) \psi_k(\delta) \rangle = y_k \gamma_k^2 \tag{6}$$

Therefore, the integral on the left side has to be evaluated and divided by the squared norm to obtain the coefficient:

$$y_k = \frac{1}{\gamma_k^2} \langle Y(\delta), \psi_k(\delta) \rangle \tag{7}$$

This approach is generally referred to as spectral projection [11]. In the case of multiple uncertain parameters ($n_\delta = N > 1$), a multivariate polynomial basis is required. We adopt a total-order expansion, in which the basis consists of all products of univariate orthogonal polynomials whose total degree does not exceed a prescribed maximum order P. This results in a basis of $\frac{(N+P)!}{N!P!}$ multivariate polynomials [11]. The approach for calculating the y_k is the same as in Eq. 7, except that for calculating the inner product, a multidimensional integral over all δ has to be calculated, and the squared norm γ_k^2 is the product of the squared norms of the univariate basis functions.

3 Problem Definition

The goal of this paper is to apply non-intrusive PCE to analyze the distribution of pointing error indices and stability margins of an existing controller for three-axis attitude tracking of the MetOp-SG satellite. In particular, the absolute performance error (APE) of the attitude as well as the gain and phase margins are approximated by PCE. Systems that can tolerate high gain-only or phase-only variations can become unstable when subject to simultaneous gain- and phase variations [12]. Therefore, maximum margins guaranteed by a stability disk are used in this paper. For the sake of brevity, we exemplary use the loop-at-a-time margins from the first input to the first output of the MIMO system to show the accuracy of our approach, leaving the other loops unperturbed. However, it can be equally used for any other margin definition. In addition to the mean and standard deviation, which are directly obtained from the PCE coefficients, a histogram of the distribution of the quantities of interest is also generated to evaluate the suitability of the PCE expansion as a surrogate model of the original system. For that purpose, the uncertain parameters are randomly sampled according to their distribution and directly inserted into the polynomial system. The results and the necessary computation time are then compared to MC simulations with an adequate number of samples.

3.1 MetOp-SG Satellite

The Met-OP SG Satellite is part of a series of three satellite pairs for meteorological Earth observation. The satellite is in a sun-synchronous orbit with an altitude of 817 km, an inclination of 99° and an orbital period of 102 min. It features a rigid central body, a solar array, and two scatterometers. The satellite is modeled as a linear system with eleven uniformly distributed uncertain parameters affecting its dynamics [13]:

Table 2 Uncertain parameters of the satellite model

Component	Parameter	Range (%)
Central body	Mass	10
	Moment of inertia	20
Fuel	Mass	23
Solar array	Mass	10
	Moment of inertia	10
	1^{st} and 2^{nd} cantilever frequency	10
2 Scatterometers	Mass	10
	Moment of inertia	20

The central body is modeled as rigid; the fuel is taken into account through its contribution to the mass and moments of inertia, but sloshing effects are not considered. For the appendages, only the two flexible modes of the solar array with the lowest frequency are considered, since they have the highest impact on the spacecraft dynamics. The controller considered in this system has been described in [13]. It aims to track a reference attitude in the spacecraft body frame by commanding a reaction wheel torque. In addition to the tracking requirement, a mixed-sensitivity scheme was used to ensure attenuation of the flexible modes, noise rejection, limitation of the control effort, as well as gain, phase and modulus margins. Although created as a Linear Parameter-Varying (LPV) controller to optimize performance throughout an entire orbit, in this work it is only evaluated at a single design point. As a result, the controller operates effectively as an LTI controller.

3.2 Pointing

The pointing error metric considered in this paper is the APE around the x-, y-, and z axis. The pointing error sources of the system are the sensor noises of the satellite's star trackers and the environmental disturbance torques. The sensor noise can be described by high and low spacial frequency error, modeled as first-order Gauss-Markov processes, and temporal error, which can be considered white noise. The disturbance is modeled as the power spectral density of the simulated disturbance torque across three orbits. Each noise and disturbance is equated to specific transfer functions W_n and W_d added at the respective locations in the system as described in [13]:

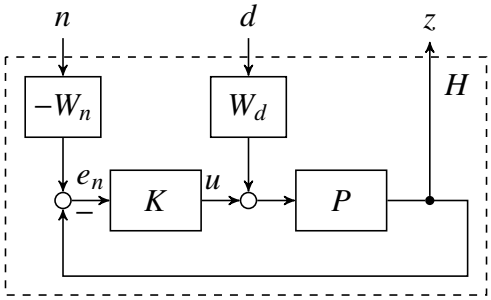

Fig. 1 Extended system for performance metric calculation

The pointing error metric which equates to the standard deviation of the output can then be computed as the H_2-norm of the transfer function H from a white noise input at n and d to the error metric z:

$$\sigma_{APE} = \sqrt{\frac{1}{2\pi}\int_{-\infty}^{\infty} \mathrm{tr}(H(j\omega)^* H(j\omega))\mathrm{d}\omega} = \|H\|_2 \tag{8}$$

Exemplary, only the pointing error around the x axis is considered below.

4 Methodology

4.1 Sparse Grid Quadrature

Recall Eq. 7 for calculating the k-th coefficient:

$$y_k = \frac{1}{\gamma_k^2}\langle Y(\delta), \psi_k(\delta)\rangle = \frac{1}{\gamma_k^2}\int_{\mathcal{D}} Y(\delta)\psi_k(\delta)w(\delta)\mathrm{d}\delta \tag{9}$$

While the squared norms γ_k^2 have a closed-form solution and are straightforward to calculate, much more effort is required to solve the multidimensional integral on the right. To integrate arbitrary functions f, in this case $f = Y(\delta)\psi_k(\delta)w(\delta)$, whose complete definition is possibly not given, the use of a quadrature rule $\mathcal{U}[f]$ is a natural choice. The integral is therefore evaluated at a set of nodal points $\{p_i\}$ and multiplied with a corresponding set of fixed weights $\{\alpha_i\}$:

$$\int_{\mathcal{D}} Y(\delta)\psi_k(\delta)w(\delta)\mathrm{d}\delta \approx \mathcal{U}[f] = \sum_{j=1}^{m} \alpha_i Y(p_i)\psi_k(p_i)w(p_i) \tag{10}$$

When applied to a multidimensional integral of a function $f(\delta_1, \ldots, \delta_N)$, the quadrature rule expands to a full tensor product. We first define a multi-index $\mathbf{i} = (i_1, \ldots, i_N) \in \mathbb{N}^N$. The full quadrature $Q[f]$ is

defined as follows [11]:

$$Q[f(\delta_1,\ldots,\delta_N)] = \mathcal{U}^{i_1}[f(\delta_1)]\otimes\cdots\otimes\mathcal{U}^{i_N}[f(\delta_N)] = \sum_{i_1=1}^{m_1}\cdots\sum_{i_N=1}^{m_N}(\alpha_{j_1}^{i_1}\otimes\cdots\otimes\alpha_{j_N}^{i_N})f(p_{j_1}^{i_1},\ldots,p_{j_N}^{i_N}) \quad (11)$$

which requires a total of $\prod_{k=1}^{N} m_k$ nodal points and function evaluations. This approach is therefore not feasible for obtaining the coefficients of PCE system with $N = 11$ uncertainties as considered in this paper with reasonable computational effort. In this case, it is common [10, 11] to employ a sparse-grid quadrature scheme as first described in [14]:

$$Q[f] = \sum_{r+1\le|\mathbf{i}|\le r+N}(-1)^{r+n-|\mathbf{i}|}\binom{n-1}{r+n-|\mathbf{i}|}\left(\mathcal{U}^{i_1}\otimes\cdots\otimes\mathcal{U}^{i_N}\right) \quad (12)$$

where $|\mathbf{i}| = i_1 + \ldots + i_N$ and r is a grid level that controls the number of nodal points in the quadrature scheme. In this paper, isotropic Gauss-Legendre quadrature weights and nodes have been used. It must be noted that for calculating the coefficients y_k according to Eq. 7, the computationally expensive function $Y(p)$ must only be evaluated once for each nodal point p and the result can be stored and used for all k. The evaluation of the polynomials ψ_k can be precomputed for later look-up once the PCE degree and grid level are defined, since they are independent of the function Y. Those properties can significantly speed up the process. The Sparse Grids Matlab Kit has been used to compute the nodal points and weights for this paper, which allows the generation of grids according to an user-defined grid level [15].

4.2 Comparison with Monte-Carlo simulations

To achieve a fair comparison of the computational efforts of PCE and MC simulations, a minimum MC sample size must be defined which is required to estimate the statistical quantities with the desired accuracy. According to the Central Limit Theorem, the distribution of the sampling mean converges to a normal distribution when the sample size approaches infinity. This allows us to determine the minimum required number of samples n_{req}, such that the sampling mean $\hat{\mu}$ lies within a relative error margin ϵ of the true mean μ with respect to a certain confidence level:

$$n_{req} = \left(\frac{z_{\alpha/2}\hat{\sigma}}{\epsilon\hat{\mu}}\right)^2 \quad (13)$$

with the standard normal quantile $z_{\alpha/2} = 1.96$ for a 95% confidence level and and chosen relative error $\epsilon = 0.01$. Since the sample mean $\hat{\mu}$ and sample standard deviation $\hat{\sigma}$ are not known a priori, they have to be estimated first by running the simulation for a large n. Besides the mean, also the standard deviation of the PCE shall be compared with the MC simulations. However, in contrast to the mean, there exists no closed-form expression to describe the convergence of the standard deviation without requiring assumptions about the underlying distribution. Therefore, an empirical approach has been used to estimate the relative error of the standard deviation with respect to a confidence level for a certain number of runs. First, a set of different sample sizes $n_i \in \mathbb{N}$ have been defined. Then, for each sample size, $B \in \mathbb{N}$ MC runs were performed and the sample standard deviations $\hat{\sigma}_b^{(n)},\ b = 1,\ldots,B$ have been calculated. The fraction of standard deviations f_n that lie within a relative error margin ϵ around the ground-truth standard deviation $\hat{\sigma}$ (obtained from a very large MC simulation) is given by

$$f_n = \frac{1}{B}\left|\left\{\hat{\sigma}_b^{(n)} : (1-\epsilon)\hat{\sigma} \le \hat{\sigma}_b^{(n)} \le (1+\epsilon)\hat{\sigma}\right\}\right| \quad (14)$$

The required sample size is the smallest tested n for which the fraction is larger than the confidence level of 95%:

$$n_{req} = \min\{n : f_n \geq 0.95\} \tag{15}$$

The relative error threshold of $\epsilon = 0.01$ and the confidence level of 95% are an arbitrary choice only valid for this test scenario and have to be adapted depending on the respective requirements. It has been found that to bound the relative error of the standard deviation, a much higher n is required compared to the error of the mean for the same confidence level. Therefore, this stricter criterion of Eq. 15 has been used to determine the required MC sample size for each quantity of interest (see Table 3).

4.3 Evaluation Setup

A maximum PCE degree of $L - 1 = 2$ together with a Legendre polynomial basis suited for the uniformly distributed parameters has been chosen. For eleven uncertainties and a total-order expansion, this results in 78 multivariate basis polynomials and corresponding coefficients. A higher polynomial degree would increase the accuracy only marginally while increasing the number of coefficients to be computed to 364. A grid level of $r = 2$ has been found sufficient to integrate the target functions accurately, resulting in 287 grid points. As explained above, this means that only 287 evaluations of the computationally expensive functions are necessary. The mean and standard deviation in Tab. 3 have been directly obtained from the coefficients according to Eq. 5 for PCE and calculated from the simulation results for MC. To prove that the polynomial expansion accurately represents the behavior of the original system, the same sample values have then be reused as an input for the PCE system as shown in Fig. 2. The margin evaluations at the integration grid points were performed using the Matlab Robust Control Toolbox.

4.4 Results

Table 3 Comparison of MC and PCE results

Metric	Method	Mean	Std	Time
APE X	PCE	2.607 µrad	0.424 µrad	3.879 s
	MC (n = 10500)	2.605 µrad	0.425 µrad	128.284 s
	Rel. Difference	0.08%	-0.24%	-95.98%
Gain margin	PCE	6.141 dB	0.424 dB	2.160 s
	MC (n = 8400)	6.142 dB	0.424 dB	41.492 s
	Rel. Difference	-0.02%	0%	-93.79%
Phase margin	PCE	31.459°	0.515°	2.204 s
	MC (n = 7700)	31.464°	0.511°	49.526 s
	Rel. Difference	-0.02%	0.78%	-94.55%

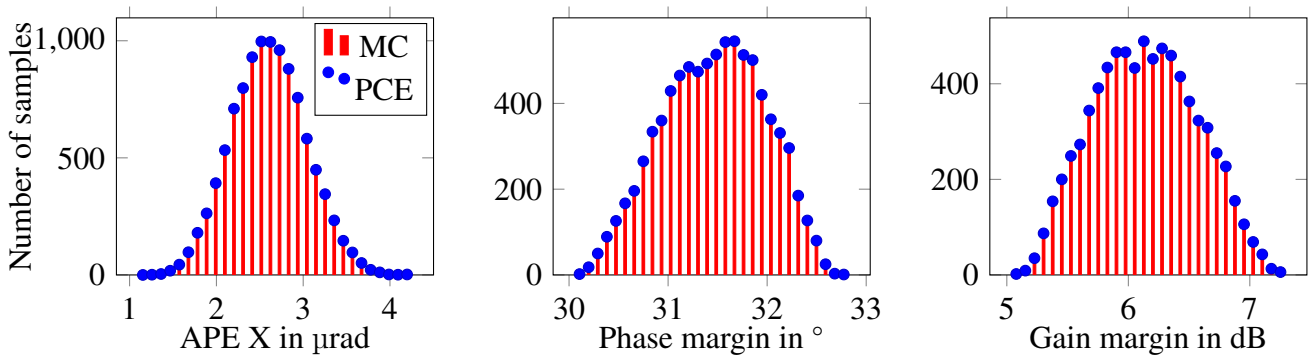

Fig. 2 Comparison of the distributions of the quantities of interest, evaluated with MC and PCE

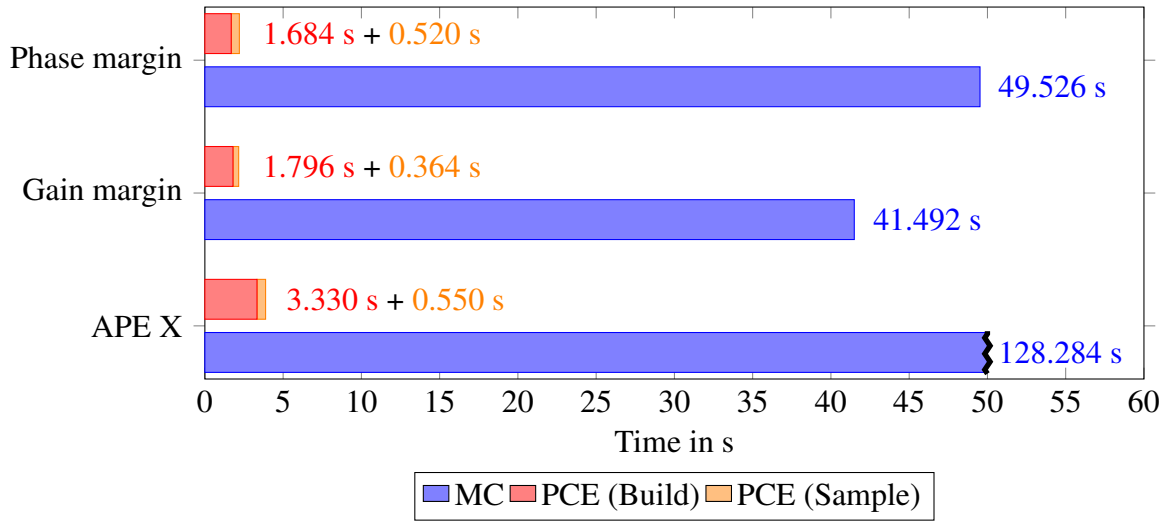

Fig. 3 Comparison of MC and PCE computation times. Note that the MC bar for the APE had to be truncated for readability

The results in Tab. 3 show a very high agreement between PCE and the MC simulations. All errors are well below 1%, which is the assumed accuracy of the MC simulations. In addition to computing the high-level metrics mean and standard deviation accurately, PCE also reproduces the system behavior for each set of sampled uncertainty parameters with near-perfect fidelity. The resulting distribution is virtually indistinguishable from the simulation of the real system, as illustrated in Fig. 2. At the same time, the total PCE computation times, combining the time for calculating the coefficients (build) and evaluating the polynomials at the sampling points (sample) are about 20 to 30 times lower than for the required number of MC runs, as shown in Fig. 3. It is important to note that once the PCE system has been built, which has to be done only once if the system and the distribution of the uncertainties do not change, the time for evaluation at one certain point of the uncertainty space becomes negligible (e.g. for the APE it took an average of roughly 5×10^{-5} seconds per sample). Once the framework for generating the PCE has been set up, any (sufficiently smooth) function of the system can be approximated with only minor changes in the code, which gives great flexibility. The non-intrusive PCE approach can be seen as a refined version of MC exploiting additional system knowledge: Instead of random points, the function of interest is only evaluated at selected points (the integration grid points) with the extra step of appropriately scaling each value based on the distribution of the uncertain parameters (by multiplying with the suitable basis polynomials and dividing by the norm squared). In this example, the maximum polynomial degree L could be easily found by iteratively increasing it until a satisfactory result was obtained. Methods for automatically choosing an optimal degree (so-called adaptive PCE) are described in the literature (e.g. [16])

5 Conclusion

This paper presented the application of non-intrusive PCE for the probabilistic analysis of stability margins and pointing of an attitude control loop for a satellite with a high number of uncertainties. It demonstrated the strong applicability of our approach. The comparison with MC simulations highlights three major advantages: A significant speed-up of the computation with excellent accuracy while keeping the flexibility to easily choose the quantity of interest. That makes PCE a powerful alternative for uncertainty analysis in the aerospace V&V process. There are two important limitations to the proposed use of PCE: it requires a smooth dependence of the quantity of interest on the parameters, and even some smooth functions (e.g., those with highly oscillatory behavior) might need a very high polynomial degree which can render the computation of the coefficients expensive. Additionally, the sparse grid quadrature does not scale well to high-dimensional problems, which can make the method intractable when dealing with a large number of uncertainties. Further work could extend the approach to LPV systems by including parameters that depend on the orbital position as additional uncertainties within the framework. This would enable capturing the system characteristics over the entire orbit. Adaptive PCE could be used to find an optimal polynomial basis with a minimum amount of manually selected parameters.

Acknowledgments

This work is partially supported by ESA Project No. 4000140610/22/NL/GLC/cb entitled New AOCS V&V Technologies for Industrial Efficiency.

Declaration of Use of Artificial Intelligence

Artificial intelligence was not used in the work presented.

References

[1] Andrés Marcos, Christophe Roux, Max Rotunno, Hans-Dieter Joos, Samir Bennani, Luis Penin, and Augusto Caramagno. The V&V problematic for launchers: current practise and potential advantages on the application of modern analysis techniques. In *Proceedings of ESA GNC, 2011*, Karlovy Vary, Czech Republic, 2011.

[2] Jean-Marc Biannic, Clément Roos, Samir Bennani, Fabrice Boquet, Valentin Preda, and Bénédicte Girouart. Advanced probabilistic μ-analysis techniques for AOCS validation. *European Journal of Control*, 62:120–129, 2021. ISSN: 09473580. doi: 10.1016/j.ejcon.2021.06.019.

[3] Xinjia Chen, J. L. Aravena, and Kemin Zhou. Risk analysis in robust control - making the case for probabilistic robust control. In *Proceedings of the 2005, American Control Conference, 2005*, pages 1533–1538, Portland, Oregon, USA, 2005. IEEE. ISBN: 0-7803-9098-9. doi: 10.1109/ACC.2005.1470185.

[4] Mario Izquierdo Serra, Maurice Martin, Simon Delchambre, Stefan Winkler, and Harald Pfifer. Probabilistic Verification of Spacecraft Acquisition Sequence Using Polynomial Chaos Expansion. In *AIAA SCITECH 2025 Forum*, Orlando, Florida, USA, 2025. American Institute of Aeronautics and Astronautics. ISBN: 978-1-62410-723-8. doi: 10.2514/6.2025-0315.

[5] Luca L. Evangelisti and Harald Pfifer. Finite-Horizon Robustness Analysis of an Automatic Landing System Under Probabilistic Uncertainty. *Journal of Guidance, Control, and Dynamics*, pages 1–9, 2023. ISSN: 0731-5090. doi: 10.2514/1.G007518.

[6] Fenfen Xiong, Ying Xiong, and Bin Xue. Trajectory Optimization under Uncertainty based on Polynomial Chaos Expansion. In *AIAA Guidance, Navigation, and Control Conference*, Kissimmee, Florida, USA, 2015. American Institute of Aeronautics and Astronautics. ISBN: 978-1-62410-339-1. doi: 10.2514/6.2015-1761.

[7] Norbert Wiener. The Homogeneous Chaos. *American Journal of Mathematics*, 60(4):897, 1938. ISSN: 00029327. doi: 10.2307/2371268.

[8] F. Augustin and P. Rentrop. Stochastic Galerkin techniques for random ordinary differential equations. *Numerische Mathematik*, 122(3):399–419, 2012. ISSN: 0029-599X. doi: 10.1007/s00211-012-0466-8.

[9] Dongbin Xiu and George Em Karniadakis. The Wiener–Askey Polynomial Chaos for Stochastic Differential Equations. *SIAM Journal on Scientific Computing*, 24(2):619–644, 2002. ISSN: 1064-8275. doi: 10.1137/S1064827501387826.

[10] Jeongeun Son and Yuncheng Du. Comparison of intrusive and nonintrusive polynomial chaos expansion-based approaches for high dimensional parametric uncertainty quantification and propagation. *Computers & Chemical Engineering*, 134:106685, 2020. ISSN: 00981354. doi: 10.1016/j.compchemeng.2019.106685.

[11] Michael Eldred and John Burkardt. Comparison of Non-Intrusive Polynomial Chaos and Stochastic Collocation Methods for Uncertainty Quantification. In *47th AIAA Aerospace Sciences Meeting including The New Horizons Forum and Aerospace Exposition*, Orlando, Florida, USA, 2009. American Institute of Aeronautics and Astronautics. ISBN: 978-1-60086-973-0. doi: 10.2514/6.2009-976.

[12] Peter Seiler, Andrew Packard, and Pascal Gahinet. An Introduction to Disk Margins [Lecture Notes]. *IEEE Control Systems*, 40(5):78–95, 2020. ISSN: 1066-033X. doi: 10.1109/MCS.2020.3005277.

[13] Emily Burgin, Felix Biertümpfel, and Harald Pfifer. Linear Parameter Varying Controller Design For Satellite Attitude Control. *IFAC-PapersOnLine*, 56(2):3112–3117, 2023. ISSN: 24058963. doi: 10.1016/j.ifacol.2023.10.1443.

[14] Sergey Smolyak. Quadrature and interpolation formulas for tensor products of certain classes of functions. In *Soviet Math. Dokl*, volume 4, pages 240–243, 1963.

[15] C. Piazzola and L. Tamellini. Algorithm 1040: The Sparse Grids Matlab Kit - a Matlab implementation of sparse grids for high-dimensional function approximation and uncertainty quantification. *ACM Transactions on Mathematical Software*, 50(1), 2024. doi: 10.1145/3630023.

[16] Géraud Blatman and Bruno Sudret. Adaptive sparse polynomial chaos expansion based on least angle regression. *Journal of Computational Physics*, 230(6):2345–2367, 2011. ISSN: 00219991. doi: 10.1016/j.jcp.2010.12.021.